Article:
Aldakheel, F., Ismail, M.S., Hughes, K.J. et al. (2021) Effects of compression on mechanical integrity, gas permeability and thermal stability of gas diffusion layers with/without sealing gaskets. International Journal of Hydrogen Energy, 46 (44). pp. 22907-22919. ISSN: 0360-3199

https://doi.org/10.1016/j.ijhydene.2021.04.087

Effects of compression on mechanical integrity, gas permeability and thermal stability of gas diffusion layers with/without sealing gaskets

F. Aldakheel [a, b *], M.S. Ismail [a, c *], K.J. Hughes [a], D.B. Ingham [a], L. Ma [a], and M. Pourkashanian [a, c]

[a] Energy 2050, Department of Mechanical Engineering, Faculty of Engineering, The University of Sheffield, Sheffield, S3 7RD, United Kingdom

[b] Energy and Building Research Center, Kuwait Institute for Scientific Research (KISR), Al-Jaheth Street, Shuwaikh Educational Area, P.O. Box 24885, Safat, 13109, Kuwait

[c] Translational Energy Research Centre (TERC), University of Sheffield, Sheffield, S9 1ZA, United Kingdom

[*] Corresponding authors: Tel: +44 114 21 57242
Email addresses: faajma1@sheffield.ac.uk (F. Aldakheel); m.s.ismail@sheffield.ac.uk (M.S. Ismail)

Abstract

The compressibility, the gas permeability and the thermal stability of 4 commercially available uncoated GDLs (or carbon substrates) and MPL-coated GDLs are, with/without Teflon and silicone sealing gaskets, investigated before and after performing ex-situ compression tests mimicking the compressive stresses within the fuel cell. The results show that the gas permeability of the tested GDLs are impacted more with Teflon gaskets than with the silicone gaskets and this is due to the lower stiffness of the former gaskets. Likewise, the GDLs are more deformed with the Teflon gaskets than with silicone gaskets and this is due to the same reason mentioned above. The thermogravimetric analysis (TGA) data suggests that the bare carbon substrates, unlike the MPL-coated GDLs, lose up to 40% of the PTFE material after the compression test either with or without sealing gaskets.

Keywords: PEM fuel cells; Gas diffusion layers; Compression; Gas permeability; Sealing gaskets; Thermogravimetric analysis

1. Introduction

Polymer electrolyte membrane (PEM) fuel cells are energy converters that directly and efficiently produce electricity, with zero-emission at the point of use. Owing to its high efficiency (~ 50%), noise-free operation and clean by-products (only pure water), PEM fuel cell is one of the promising power conversion technologies for a multitude of portable, automotive and stationary applications. One of the essential components inside PEM fuel cells is a gas diffusion layer (GDL). GDLs are mainly responsible for supplying the reactants (i.e. O_2 and H_2) from the flow channels grooved in the flow-field plates to the active areas in the catalyst layers as uniformly as possible [1]–[3]. Additionally, GDLs transport electronic charge and heat between the catalyst layers and the flow field plates and act as a mechanical support to the delicate catalyst layers. Further, they are typically coated with hydrophobic microporous layers (MPLs) to improve the electrical contact with the catalyst layers and to assist in rejecting excess water generated at the cathode side of the fuel cell [4], [5].

There are different factors that play a significant role in affecting the mass transport properties of the GDLs (e.g. gas permeability and diffusivity). The GDL is subject to two types of degradation: mechanical degradation (due to the stresses acting on the GDLs) and chemical degradation (due to the erosion and corrosion taking place within the environment of the fuel cell). It should be noted that these forms of degradation are not limited to the GDLs and could be seen with the other components of the fuel cell such as the bipolar plates. For example, Li et al. [6] found that, through conducting durability tests for a high-temperature PEM fuel cell, the degradation in fuel cell performance reduces to almost zero if the used stainless steel plates are coated with stacked layers of chromium nitride and chromium. This is evidently due to the reduction in the chemical degradation of these plates that were coated with corrosion-resistant layers. On the other hand, the

degradation in fuel cell performance in the case of bare stainless steel or graphite bipolar plates is around 16%.

There are two types of mechanical stresses (or compressions or pressures) that the GDL normally undergoes: a constant stress dictated by the assembly of the fuel cell (assembling compression), and a cyclic stress arising from the cycles of swelling (in case of membrane hydration) and shrinkage (in case of membrane dehydration) [7]. The effects of the assembling compression on the fuel cell performance have been investigated by many research groups [8]–[12]. Overall, they found that there exists an optimum compression at which the fuel cell performance is maximised and this lies normally between 1 and 2 MPa. Too low compression pressure does not create good contact between the key components of the fuel cell, in particular between the GDLs and the flow field plates. On the other hand, too high compression significantly decreases the porosity of the porous media (GDLs), resulting in increased mass transport losses due to inadequate supply of reactants to catalyst layers and/or poor rejection of liquid water. What follows shows the key findings of some of the relevant investigations. Mason et al. [11] investigated the effects of compression on the PEMFC performance and found that the mass transport losses increase as the compression increases from 0.5 to 2.5 MPa, resulting in a lower limiting current density. Ous and Arcoumanis [12] found that excessive compression (> 4 MPa) drastically increases the mass transport losses, leading to a much reduced limiting current density. Zhou et al [13] investigated the effects of a compression (0.58 - 2.43 MPa) on a fuel cell performance and found that the output power of the fuel cell is a maximum at 1.62 MPa.

The level of compression that the GDL undergoes is somewhat regulated by the presence of the sealing gaskets and this is obviously due the relatively high porosity of the GDL which could be as high as 90% [14][15]. This regulation of compression induced by the sealing gasket could prove useful as the mass transport of the GDL material are, with sealing gaskets, not badly affected due

to compression. The primary function of the sealing gaskets is, as implied by their name, to seal the fuel cell and prevent gas leakage at either side of the fuel cell. The sealing gaskets should be sufficiently strong to withstand the compressive pressures applied to the fuel cell and should ideally at the same time allow for good contact between the flow field plates and the gas diffusion layers [16]. They should also be chemically stable to resist for example the corrosive environment at the cathode side [17]. The literature shows a good number of research studies that have been conducted to investigate the mechanical or the chemical properties of the sealing gasket materials used in PEM fuel cells. Li et al. [18] studied the chemical degradation of the silicone rubber gaskets using five different aging solution with different concentrations. The aging process was up to 2500 hours. The XPS and ATR-FTIR spectroscopy showed that the surface of the silicone rubber gaskets experienced significant changes (e.g. cracks) as a sign of the deterioration of the material of the sealing gasket.

Tan et al. [19] investigated the chemical and mechanical durability of four different commercial sealing gaskets (Silicone S, Silicone G, EPDM, and FL) under fuel cell operating conditions. A regular (98% H_2SO_4 dissolved in balance in balance reagent grade water) and accelerated durability test or ADT (48% HF dissolved in balance in balance reagent grade water) solutions and three bending angles (0, 90 and 120°) were used for the test. Tan et al. [13] showed that both silicone gaskets have a mass loss and cracks in the regular and ADT solutions. However, the EPDM and FL gaskets only showed degradation after 45 days of their exposure to the ADT solution at a bending degree of 120°. On another study, Tan et al. [22] found that degradation rate of the silicone gaskets increases with increasing temperature as evidenced by the weight loss measurements at 60 °C (~ 1 %) and 80% (~ 3%) after a 12-week durability test. Ghosh et al. [20] investigated different clamping forces with two types gaskets using contact pressure distribution films. The purpose of the study was to identify the influence of gaskets, varying in material and thickness, on the contact between the GDL and the flow field plate. Results showed that the spacing between the gasket and the GDL

should be reasonable (≤ 0.2 mm) in order to achieve a good contact between the GDL and the flow field plate. Lin et al. [21] experimentally investigated the effect of gasket thickness (0.05 – 0.48 mm) with two different types of carbon cloth GDLs (NC14 and OC14) on the overall performance of the cell. The results showed that the optimum compression ratios for NC14 and OC14 GDLs that maximises the fuel cell performance are 59% and 64%, respectively.

Another important, but related, topic is the effect of the compression on the structure of the GDLs. Few examples are given. Banerjee at al. [22] investigated the effect of compression on the porosity distribution of the GDL using means of X-ray computed tomography. They found that rib compression has almost no impact on the microporous layer. Nitta et al. [23] studied the effect of compression on the GDL thermal conductivity and the contact resistance between GDLs and graphite plates. They showed that the GDL thermal conductivity is almost insensitive to the compression applied (0-5.5 MPa). Of particular interest is the impact of compression on the loading of the hydrophobic agent (e.g. PTFE). The GDL should be reasonably hydrophobic in order to be capable of rejecting excess liquid water that may hinder the flow of the reacting gas to the catalysts layer. It was shown in our previous work the contact angle, which is a measure on how hydrophobic the GDL is, decreases by up to 10% after applying compressive stresses generated by a universal testing machine [24].This is probably partly due the PTFE layers being stripped from the carbon fibres of the GDL. To this end, it would be of interest to explore the effects of compression on the PTFE loading of the GDL in the absence/presence of sealing gaskets. Thermogravimetric analysis (TGA) has been successfully employed to quantify the amount of PTFE in various types of GDL materials [25]–[28].

In this paper, we investigate, for the first time, how the sealing gaskets could affect the mass transport properties of the GDL. However, we focus on how the GDL gas permeability, which is more convenient to estimate compared to for example gas diffusivity, changes before and after

compression and with/without sealing gaskets. Both gas permeability and diffusivity of the GDL scale with porosity and therefore the changes in the gas diffusivity due to compression are expected to follow the same trends of the gas permeability. Further, to investigate the structural integrity of the GDL after applying compression in presence/absence of sealing gaskets, TGA is performed. TGA is specifically used to quantify the amount of PTFE loss as a result of compression.

2. Methodology

2.1. Materials

Four different commercial GDL materials and two different types of gaskets were used in this study. The sheets of the selected two gasket materials have the same thickness, ~ 0.25 mm, but are made from different materials: Teflon and silicone HT-6135 (Rogers Corporation, USA). Table 1 shows the investigated GDL materials, their initial thicknesses, porosities and PTFE loadings (in the carbon substrate and, if applicable, the microporous layers or the MPLs). Each set mentioned in the table consists of 5 one-inch diameter GDL material samples and the numbers 1, 2 and 3 refer to the set of samples being tested: without using gaskets, with Teflon and silicone gaskets, respectively.

Table 1 Initial thickness (measured), PTFE loaidng and porosity (as reported in the liteature) of the tested GDL materials.

GDL material	Initial Thickness (µm) [(a)]	PTFE Loading (%)	PTFE Loading of MPL (%)	Porosity (%)
SGL-34-BA	Set 1: 265.8 ± 4.0	5	NA	81 [29]
	Set 2: 268.3 ± 3.7			
	Set 3: 266.0 ± 4.4			
SGL-34-BC	Set 1: 306.0 ± 3.2	5	25	75 [29]
	Set 2: 301.3 ± 4.2			
	Set 3: 303.8 ± 3.3			
SGL-39-BA	Set 1: 251.8 ± 3.4	5	NA	89 [29]
	Set 2: 253.5 ± 3.4			
	Set 3: 253.5 ± 3.6			

SGL-39-BC	Set 1: 300.0 ± 2.9	5	25	82 [29]
	Set 2: 286.5 ± 2.9			
	Set 3: 297.0 ± 3.3			

[(a)] The errors are based on the 95% confidence interval around the mean thickness of 5 samples

It should be noted that SGL 34BA and SGL 39BA are both non-woven carbon substrates; however, they are, as implied by their porosity values, of different structures. SGL 34BA is probably, with the lower-porosity, more suitable for low-humidity operating conditions than the SGL 39BA [30].

2.2. Mechanical characterisation

The compression test for both the GDLs and gaskets was conducted using a universal testing machine, Shimadzu EZ-LX (Shimadzu corporation, Japan). The readings obtained were corrected for machine compliance as described in [31]. To investigate the effects of the gaskets on the compressibility of the GDL materials, the GDL samples of the first set (i.e. Set 1) and the gasket samples were separately tested for compression. The GDL samples of the second or the third set (i.e. Set 2 or Set 3) were then tested for compression in combination with the Teflon or silicone gasket materials; see Figure 1(a). The diameter of the GDL sample is 1.0 inch and the outer diameter of the annular gasket sample encircling the GDL sample is around 1.5 inch. As detailed in [24], the test was designed to simulate the various compression types that the GDL materials subjected to inside the housing of the fuel cell, namely: (i) the assembling compression and (ii) the cyclic loading and unloading compressions arising from the hydration and the dehydration of the membrane electrolyte. It should be noted that the compression on the GDL due to the swelling of the membrane could be up to 2 MPa [24], [32]. To this end, the total compression applied to the GDL samples was set to 3 MPa (1 MPa representing assembling compression plus 2 MPa due to membrane swelling). Figure 1(b) shows the sequence of the compression test with time: the first third of the loading stroke (0 to 1 MPa) represents the assembling compression and the following 1 to 3 MPa cyclic compressive strokes represent the loading and the unloading compressions the GDL undergoes due

to the swelling (due to hydration) and the shrinkage (due to dehydration) of the membrane electrolyte.

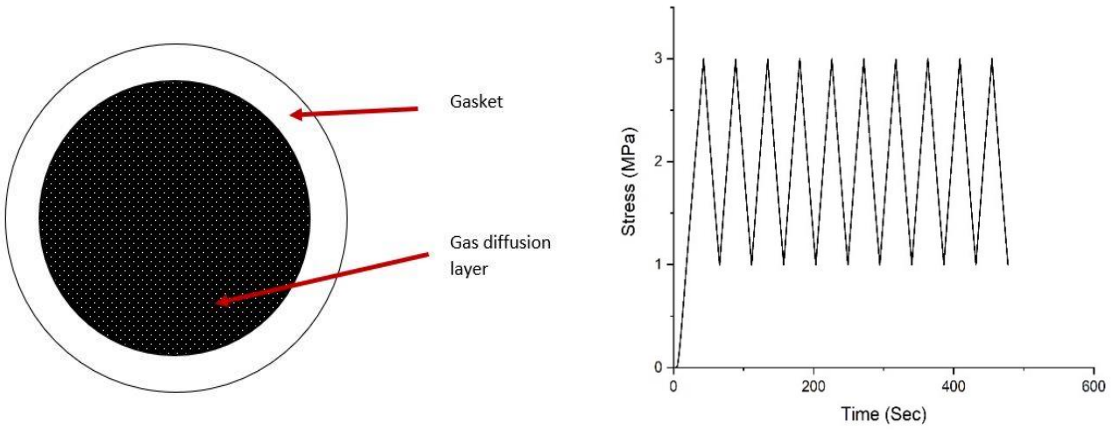

(a) **(b)**

Figure 1 (a) A schematic showing the top view of the combination of the circular GDL sample and the annular gasket sample and (b) the pattern of the compression test used on the tested GDLs and gaskets.

2.3. Through-plane gas permeability test

The gas permeability of the GDL samples before and after compression test was estimated using an in-house gas permeability setup which comprises of upper and lower fixtures as shown in Fig. 2. Circular GDL samples, with 25.4 mm diameter, are firmly placed between the two fixtures [33]–[37]. A 0.1 lit/min mass flow controller (HFC-202, Teledyne Hastings, UK) was used to control the flow rate of nitrogen gas over the GDL samples. Five to seven incremental flow rates were used for each test and the pressure drop across the sample was measured for each flow rate using a highly sensitive (~ 12 Pa) pressure transducer (PX653, Omega, UK).

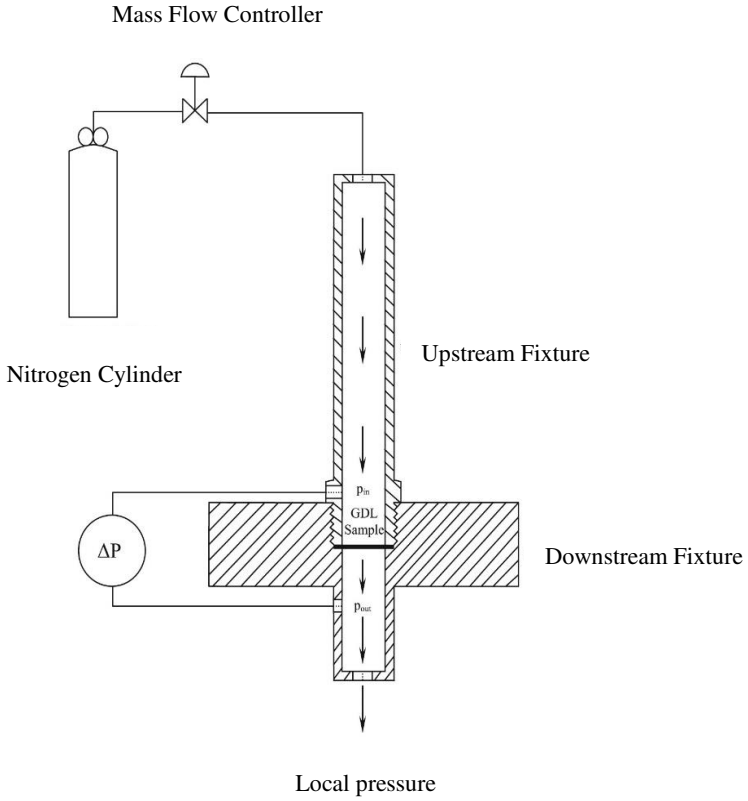

Figure 2 A schematic of the gas permeability set-up. Reproduced with permission from Elsevier from [21].

The resulting pressure gradient – flow rate curves were shown to be almost linear (see Fig. 3). Subsequently, the inertial losses were assumed to be negligible and Darcy's law was used to estimate the through-plane gas permeability of the GDL samples:

$$\frac{\Delta P}{L} = \frac{\mu}{K} u \tag{1}$$

$$u = \frac{Q}{\pi D^2/4} \tag{2}$$

where ΔP is the pressure difference across the GDL sample, L is the measured thickness of the sample, μ is the dynamic viscosity of the flowing gas (i.e. nitrogen) which is about 1.8×10^5 Pa.s at 20 °C, K is the gas permeability of the GDL sample, u is the velocity of the flowing gas, Q is the volumetric flow rate and D is the diameter of the GDL sample (1 inch).

Fig. 3 shows the pressure gradient as a function of gas velocity for the SGL-39-BA samples before and after compression test: (a) without using gaskets (Set 1), (b) with Teflon (Set 2) and (c) silicone (Set 3) gaskets. The experimental data were linearly curve-fitted to obtain the slope of the curve (μ/K) to estimate the gas permeability of the sample using Equation (1). It is noteworthy that the error bars in Fig. 3 represent the 95% confidence intervals around the mean values of the pressure gradients.

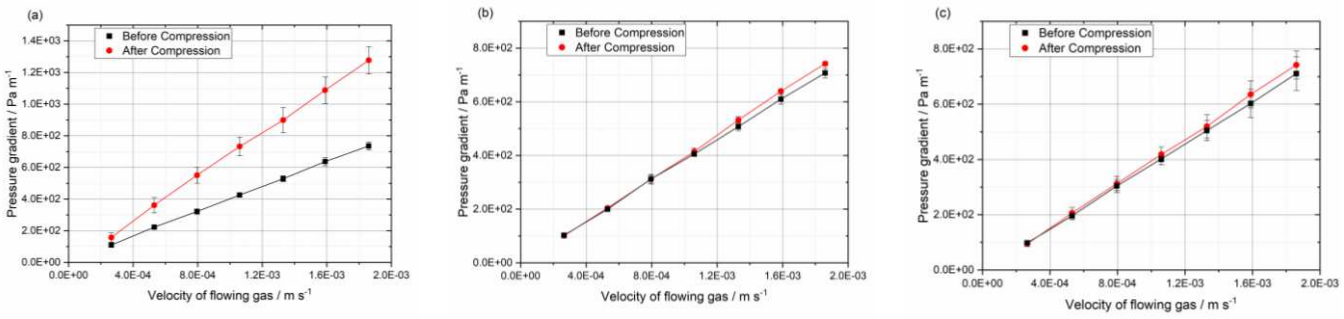

Figure 3 Pressure gradient versus gas velocity experimental data before and after compression for SGL-39-BA samples before and after compression: (a) without using gaskets (b) with Teflon gaskets and (c) with silicone gaskets.

2.4. Thermogravimetric Analysis (TGA)

Pyris 1 TGA Thermogravimetric Analyzer (PerkinElmer, USA) was used at a heating rate of 10 °C/min and under a nitrogen flow rate of 20 ml/min. This step was conducted to ensure that oxidation of the tested samples does not take place. The samples were initially exposed to nitrogen flow for 15 minutes at a temperature of 30 °C. TGA analysis is then performed as the sample is heated from 30°C to 900°C at the above-mentioned rate (i.e., 10 °C/min).

3. Results and discussion

3.1. Compression test

Fig. 4 shows the stress-strain curves for the investigated GDL materials as they were (a) without a gasket, (b) with Teflon and (c) with silicone gaskets. Namely, the hysteresis (i.e., the difference between the forward curve (loading) and backward curve (unloading) is significant for the first

cycle and becomes much less significant for the subsequent cycles. As explained in [24] , this means that the first compression, caused by cell assembling, is responsible for most of the GDL deformation. This also means that the amount of heat dissipation resulting from the internal friction (the area enclosed between the forward and backward paths) in the first cycle is the maximum [38]. Subsequent cycles of loading (due to membrane hydration) and unloading (due to membrane dehydration) contribute much less to the deformation of the GDL, resulting in much less energy dissipation and signalling that the tested material has almost mechanically reached the equilibrium (or saturation) state [24]. As shown in Fig. 4b and 4c, the gaskets have an effect on the mechanical behavior of the GDL material. Namely, the GDL material in general becomes more resistive to the compression in the presence of the gaskets; for example, the strain at the maximum applied stress, i.e. 3 MPa, for SGL 34BA is less than 0.4 in the presence of the gaskets whereas it is around 0.45 in the absence of the gaskets. This is, compared to the GDL materials, obviously due to the high mechanical resistance demonstrated by the tested gasket materials; see Fig. 5. Notably, the GDL samples with Teflon gaskets show less hysteresis than those with silicone gaskets; this is in accordance with the stress-strain curves of the investigated gaskets where the Teflon gaskets demonstrate less hysteresis compared to silicone gaskets (Fig. 5). It should be noted that the thicknesses of used gaskets did not change after the compression test. It can be seen from Fig. 4 that the MPL-coated GDL materials are more resistive than their corresponding carbon substrates; to illustrate, the strain displayed by SGL 34BA at 3 MPa is around 0.45 whereas it is around 0.37 for SGL 34BC at the same stress. This is mainly attributed to the fact that the MPL-coated GDL represent a system of two mechanical resistances in series and therefore the mechanical resistance is expected to increase. Further, an “inter-phase” layer is formed between the carbon substrate and the MPL as a result of MPL penetration into the substrate [30]. This layer is made up from the MPL material and carbon fibers and acts as a reinforcing material. Consequently, this is expected to improve the overall stiffness of the GDL [31].

1

GDL	(a) Without gaskets	(b) With Teflon gaskets	(c) With silicone gaskets
SGL 34-BA	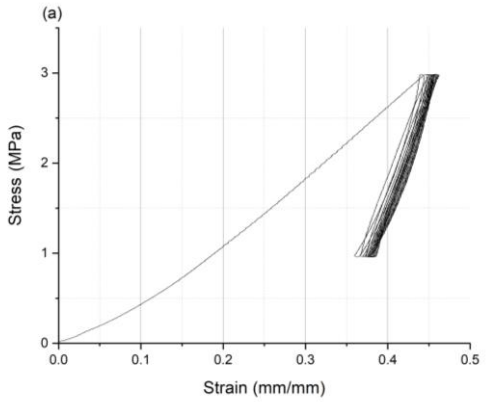	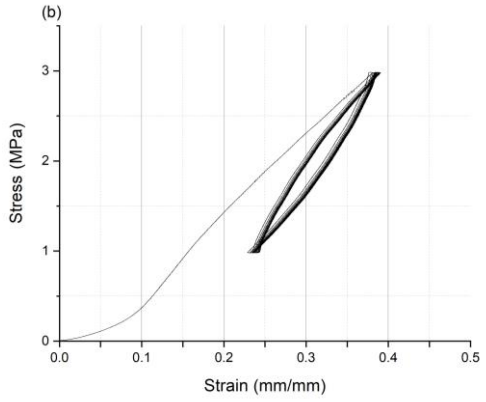	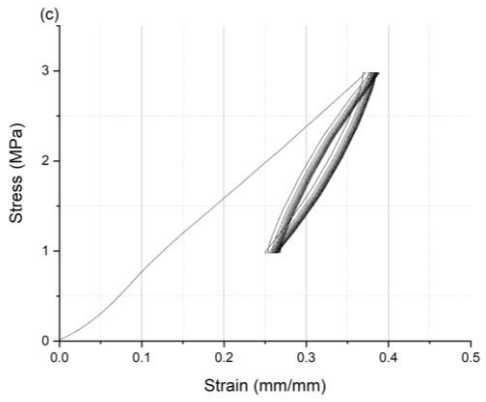
SGL-34-BC	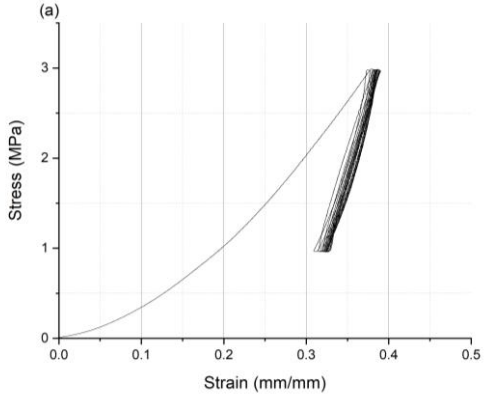	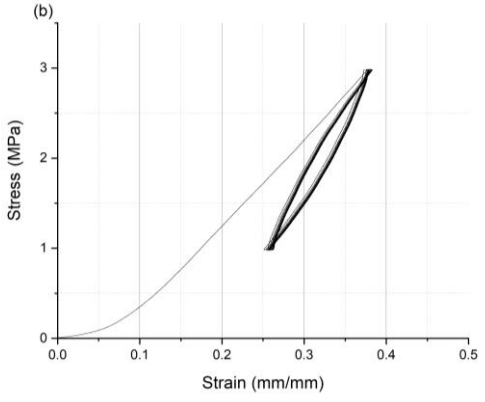	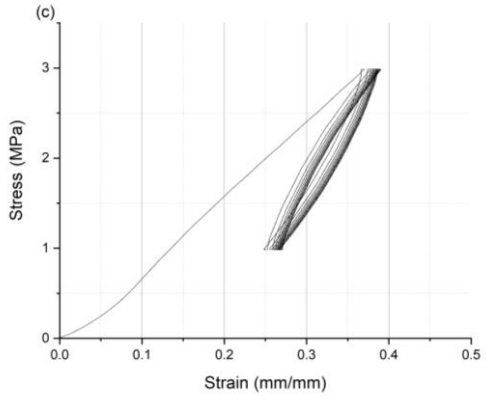

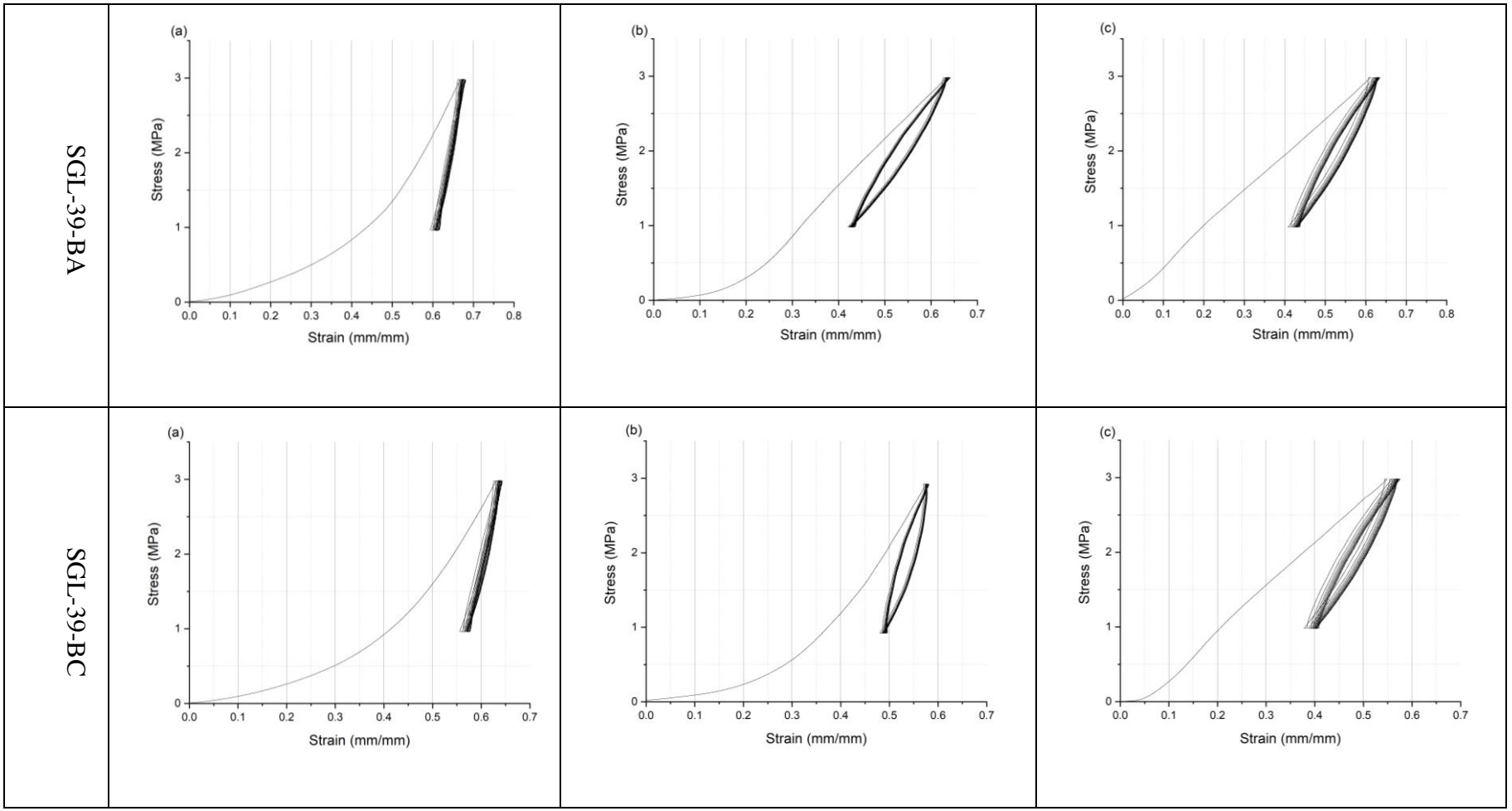

Figure 4 The stress-strain curves of the tested GDL materials (a) without gaskets, with (c) Teflon gaskets and (d) silicone gaskets.

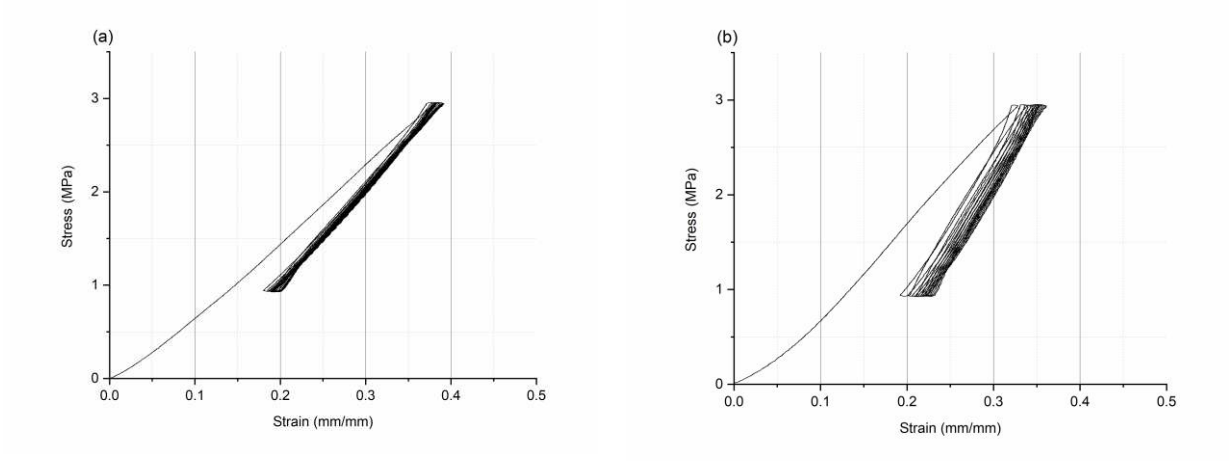

Figure 5 The stress-strain curves for typical samples of (a) Teflon and (b) silicon gaskets.

3.2. Gas permeability

The gas permeability of the tested GDL samples were experimentally estimated before and after compression tests in order to primarily evaluate the effects of the presence of the sealing gaskets. Table 2 shows the gas permeability of the samples before and after compression tests. It also shows the amount of reduction in permeability and thickness after performing the compression tests. Further, bar charts were generated for the gas permeability values to allow the readers to readily recognise the impact of compression on the gas permeability of the GDL samples (Fig. 6). As expected, the permeability and the thickness of the GDL samples that were subject to compression without encircling gaskets (i.e. Set 1) demonstrate significantly higher reduction in gas in thickness and gas permeability compared to those encircled with Teflon and silicone gaskets respectively (i.e. Sets 2 and 3). This is evidently because the gaskets, owing to their higher stiffness relative to GDL samples, limit the extent to which the GDL samples are compressed. For example, the mean thickness and permeability of SGL 34BA samples, which were not encircled by annular gaskets when subjected to compression, have reduced by about 16 and 18%, respectively, after

compression. On the other hand, the mean thickness of the GDL samples, encircled by silicone gaskets when subjected to compression tests (i.e. Set 3), has slightly reduced (slightly above 3%) and their mean gas permeability has hardly changed after compression. Fig. 7 shows the cross-section SEM images of the investigated GDL samples before (a) and after exposed to compression (b) without gaskets, (c) with Teflon and (d) silicone gaskets. These micrographs clearly show the controlling effect of the used gaskets on the final thicknesses of the GDL samples; compare the images listed in column (b) with those listed in columns (c) and (d). The second observation is that the silicone gaskets, although they have more or less the same thickness as the Teflon gaskets, renders the thickness and the gas permeability of the GDL samples to be less reduced compared to those tested with Teflon gaskets. This is, as could be inferred from Fig. 5, attributed to the higher mechanical resistance featured by the silicone gaskets compared to Teflon gaskets. The third observation is that the MPL-coated GDL materials (i.e. SGL 34BC and SGL 39BC) demonstrate higher reductions in the mean thickness and gas permeability compared to their counterpart carbon substrates (i.e. SGL 34BA and SGL 39BA). This is more to do with the fact that the coated GDLs (SGL 34BC and SGL 39BC) experience, as a result of compression, the penetration of the MPL into the body of the carbon substrate. The MPL is much lower in porosity than the hosting carbon substrates and hence a good portion of the void fraction in the carbon substrate is replaced with the compression-induced penetrating MPL material, thus resulting in a much reduced gas permeability compared to the uncoated GDLs. Notably, one of the tested carbon substrates (i.e. SGL 39BA) is more compressible than the other (i.e. SGL 34BA) and this is due the lower density and higher porosity characterising the former carbon substrates [29], [30]; this could be also deduced from the superficial SEM images of the above two carbon substrates, namely: larger pores at the surfaces displayed by SGL 39BA; see Fig. 8. As expected, the MPL-coated GDLs follow the same trend as the corresponding carbon substrates: SGL 39BC is more compressible than SGL 34BC. It should be noted that SEM surface images for the tested GDL materials before and after compression were

not presented as there were no noticeable differences in the superficial morphology of the GDL sample before and after applying the compression. This is most likely due to the use of flat and smooth compressing plates and that most of the deformation is internal.

Table 2 Through-plane permeability before and after compression, and the percentage of both reduction in thickness and permeability. Set 1: without gaskets; Set 2: with PTFE gaskets; Set 3: with silicone gaskets.

GDL	Through-plane permeability before compression (m^2)	Through-plane permeability after compression (m^2)	Reduction in thickness (%)	Reduction in permeability (%)
SGL-34-BA Set 1:	$1.20 (\pm 0.09) \times 10^{-11}$	$9.88 (\pm 1.94) \times 10^{-12}$	15.8	17.7
Set 2:	$1.11 (\pm 0.04) \times 10^{-11}$	$1.10 (\pm 0.09) \times 10^{-11}$	5.55	0.9
Set 3:	$1.13 (\pm 0.08) \times 10^{-11}$	$1.13 (\pm 0.05) \times 10^{-11}$	3.29	0.0
SGL-34-BC Set 1:	$2.63 (\pm 0.90) \times 10^{-14}$	$1.58 (\pm 0.59) \times 10^{-14}$	14.3	39.9
Set 2:	$2.90 (\pm 1.29) \times 10^{-14}$	$2.48 (\pm 1.08) \times 10^{-14}$	7.39	14.5
Set 3:	$3.05 (\pm 1.40) \times 10^{-14}$	$2.67 (\pm 1.20) \times 10^{-14}$	5.76	12.5
SGL-39-BA Set 1:	$4.51 (\pm 0.20) \times 10^{-11}$	$2.65 (\pm 0.26) \times 10^{-11}$	34.9	41.2
Set 2:	$4.71 (\pm 0.16) \times 10^{-11}$	$4.52 (\pm 0.09) \times 10^{-11}$	4.64	4.03
Set 3:	$4.76 (\pm 0.49) \times 10^{-11}$	$4.57 (\pm 0.44) \times 10^{-11}$	3.25	3.99
SGL-39-BC Set 1:	$1.80 (\pm 0.18) \times 10^{-13}$	$3.77 (\pm 0.47) \times 10^{-14}$	29.8	79.1
Set 2:	$1.60 (\pm 0.19) \times 10^{-13}$	$1.26 (\pm 0.14) \times 10^{-13}$	7.05	21.3
Set 3:	$1.76 (\pm 0.29) \times 10^{-13}$	$1.45 (\pm 0.27) \times 10^{-13}$	6.48	17.6

1

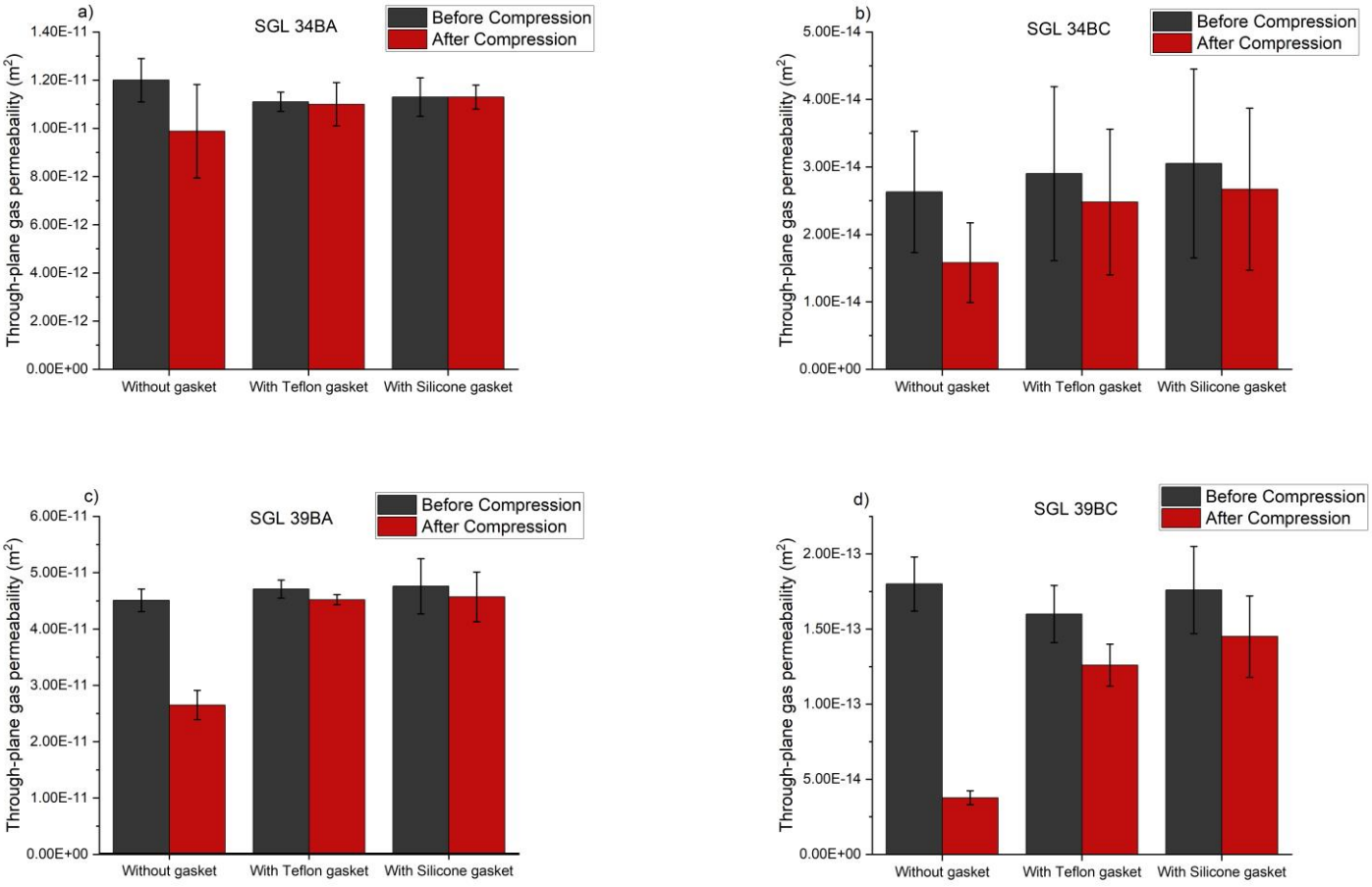

Figure 6 The through-plane gas permeability of the invetigated GDL materials before and after compression.

GDL	(a) Before compression	After compression		
		(b) Without gaskets	(c) With Teflon gaskets	(d) With silicone gaskets
SGL-34-BA	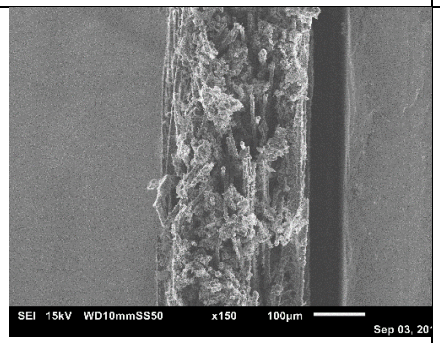	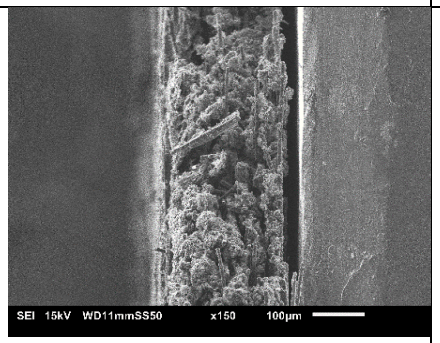	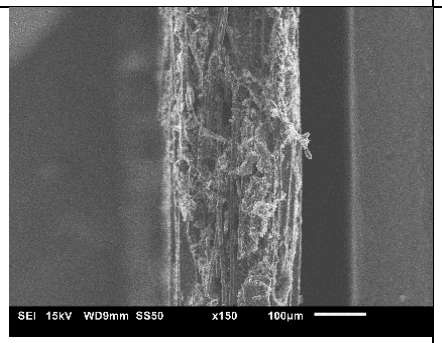	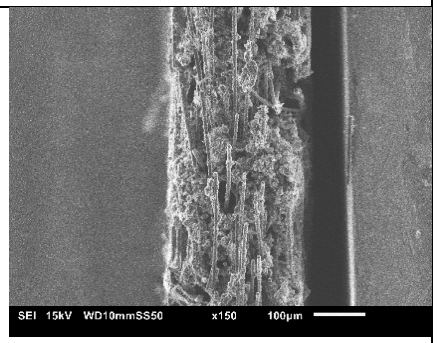
SGL-34-BC	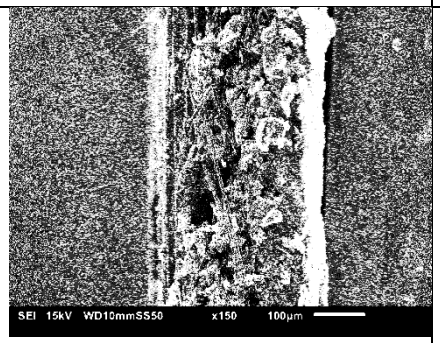	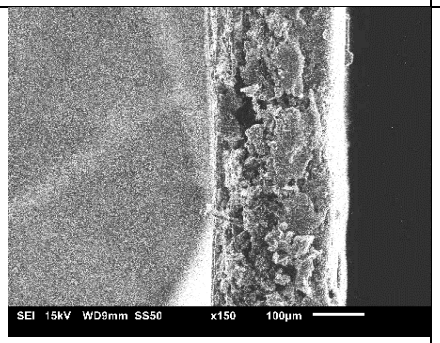	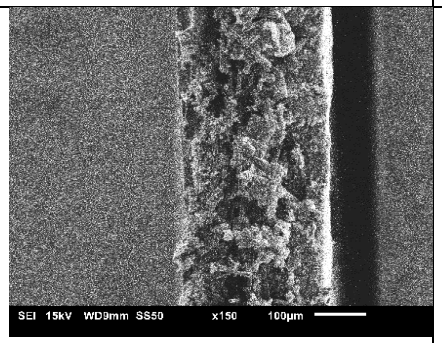	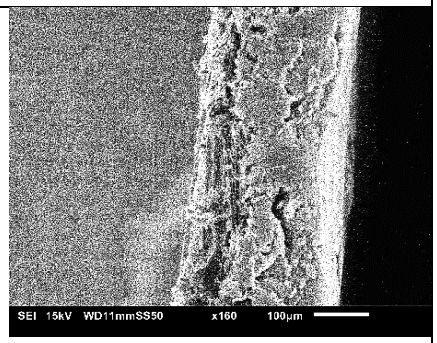

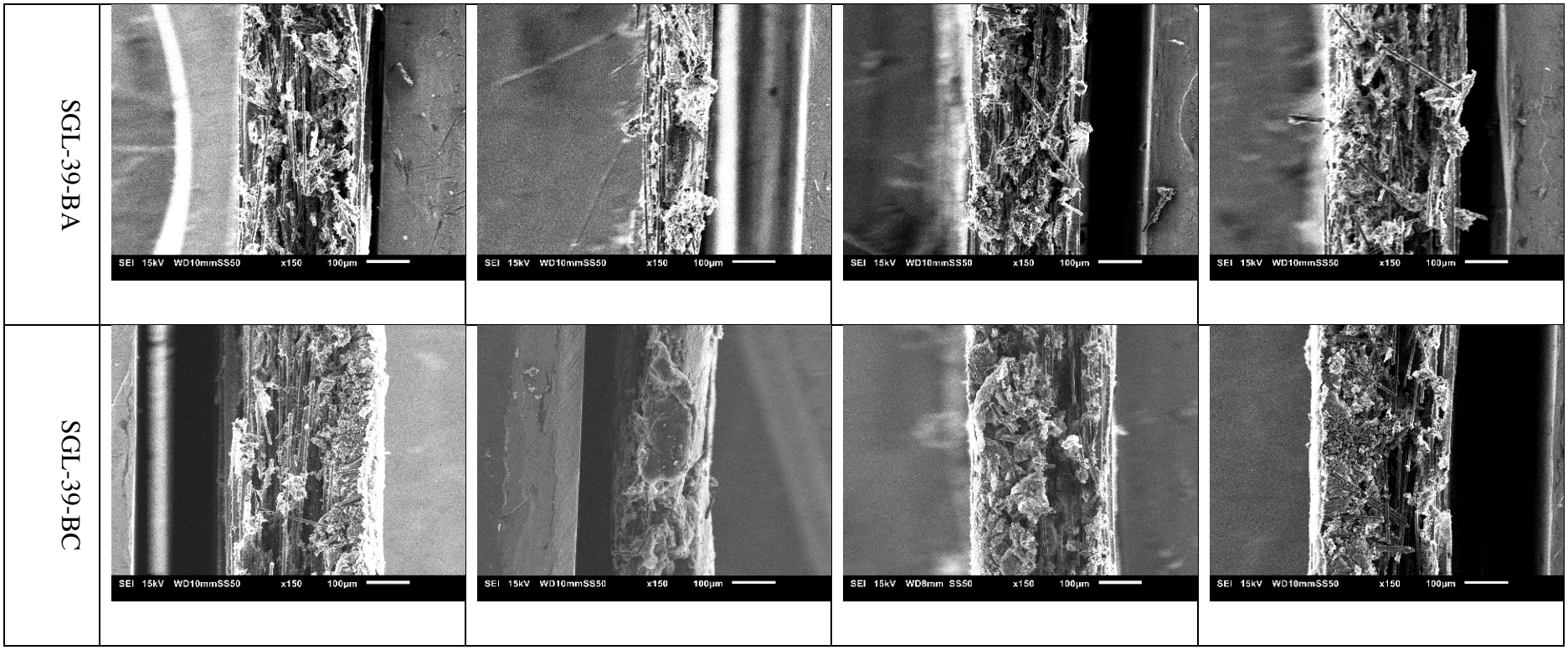

Figure 7 Cross-section SEM images of the tested GDL materials (a) before and after compression (b) without gaskets, with (c) Teflon gaskets and (d) silicone gaskets.

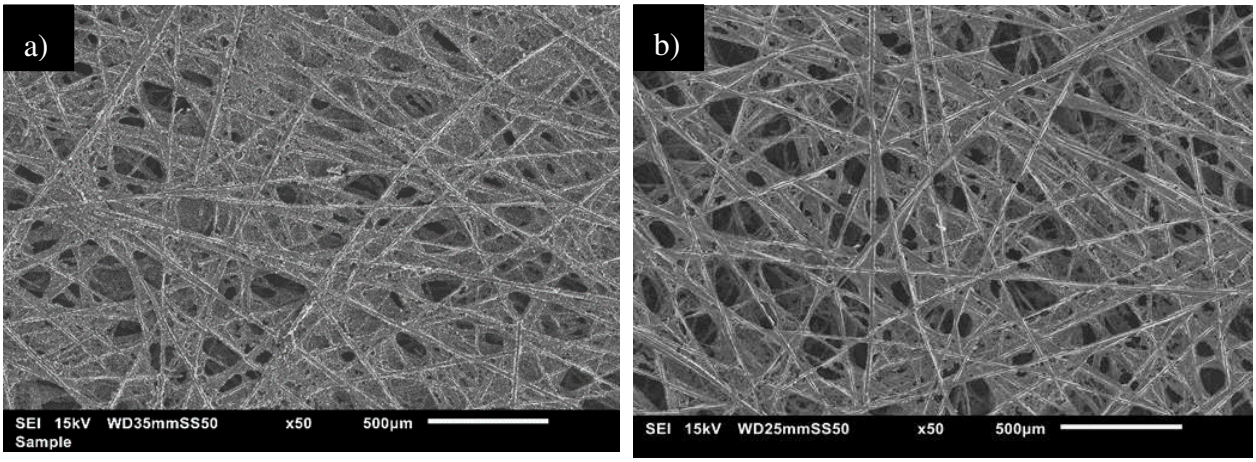

Figure 8 SEM surface images for (a) SGL-34-BA, and (b) SGL-39-BA at a magnification of 50x

3.3. Thermogravimetric analysis

Fig. 9 shows the TGA results for the tested GDL materials before and after compression. The PTFE material normally decomposes at around 600 °C [25] and therefore TGA could give an estimate of the amount of PTFE available in the tested GDL materials. Assuming that all the materials decomposing at ~ 600° is PTFE, the TGA of the uncompressed carbon substrates SGL 34BA and SGL 39BA suggests that the amount of PTFE in these GDL is around 12 wt. % (Fig. 9a and Fig 9c). Following the same assumption, the amount of PTFE in the uncompressed MPL-coated GDL materials SGL 34BC and SGL 39BC is slightly higher: ~ 15 wt. % (Fig. 9b and Fig 9d) and this is apparently due to presence of further PTFE material in the MPLs. The amount of PTFE in the carbon substrates SGL 34BA and SGL 39 BA, after compression, reduce from 12 wt. % to around 7 wt. % signaling that some PTFE material was lost during the compression; this observation is applicable to all the sets of samples (i.e. compression in absence of gaskets or compression in presence of Teflon/silicone gaskets). This is in line with some previous findings (e.g. [39] [40]) where the compression was found to cause the PTFE amount in the GDL to be reduced and this due to the

breakage of carbon fibres and/or the PTFE layers coating these fibres, particularly those located under the ribs of the bipolar plates.

However, the MPL-coated GDL materials behave differently; their PTFE loading is almost maintained after compression. This is probably due to positive impact of the MPL in terms of absorbing the compressive forces and subsequently mitigating the breakage of the PTFE bonds. This is in accordance with the findings of [22] where it was found that the compression has almost no effect on the MPL, thus corroborating our previous thought that the MPL acts as an absorbing and protective layer to the GDL sandwich.

For a given temperature after 600 °C, the weight loss of the compressed samples is less than that of the uncompressed samples; this is most likely due to that the compression makes the GDL samples lose more decomposable materials (e.g. the binding resin [41]). This statement is supported by the observation that, for a given temperature after 600 °C, the weight loss of the GDL samples compressed with silicone gaskets is in general more than those compressed with Teflon gaskets and this is apparently due to the higher stiffness demonstrated by the former gaskets which allows for less breakage and subsequent less loss of the decomposable material.

The TGA test was also performed for the tested gaskets (Fig. 9e). The results confirmed that the Teflon gaskets used are pure as there was no material left after 600 °C. They also show that the Teflon gaskets are more thermally stable than the silicone gaskets in the range between 200 and 600 °C. This signifies the suitability of the Teflon gaskets for the fuel cells that operate within the above temperature range, such as phosphoric acid fuel cells (PAFCs). It is important to note that the operating temperature of PEM fuel cells is normally less than 100 °C, and therefore the thermal stability of either Teflon or silicone gaskets is not an issue.

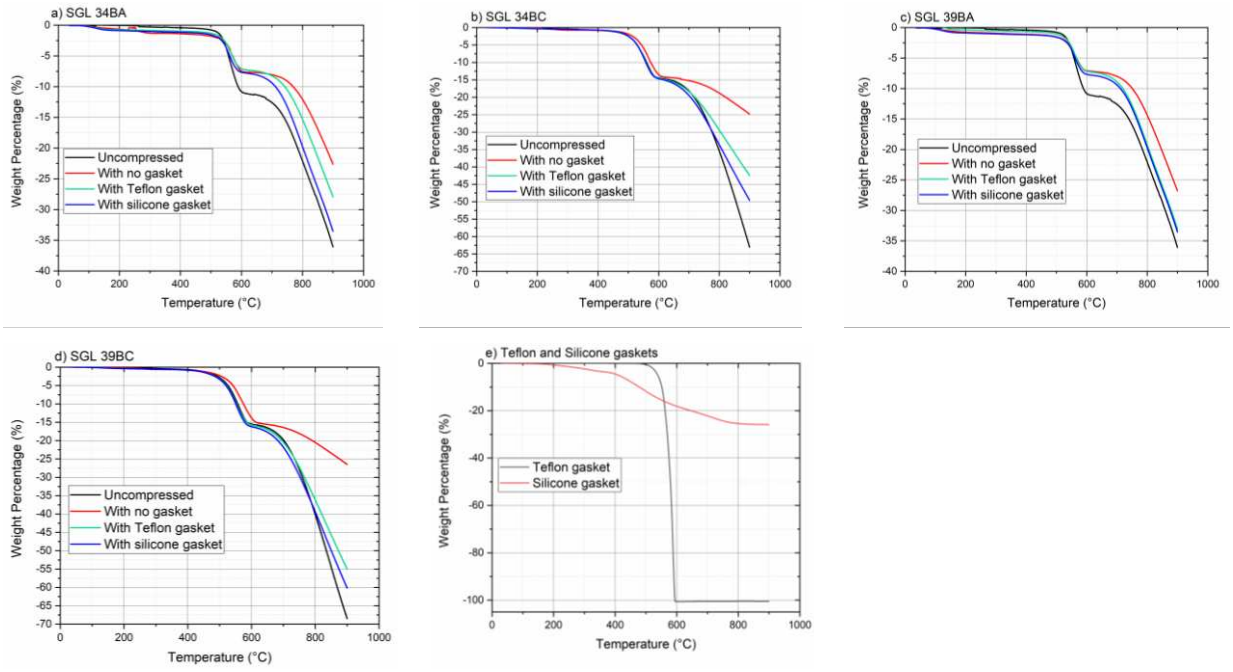

Figure 9 TGA data for (a) SGL 34BA, (b) SGL 34BC, (c) SGL 39BA, (d) SGL 39BC and (e) Teflon and silicone gaskets.

4. Conclusions

The compressibility, the gas permeability and the thermal stability of two uncoated GDLs (or carbon substrates) and two MPL-coated GDLs have been investigated before and after preforming ex-situ realistic compression tests (mimicking the compressive stresses the GDL experience within the fuel cell housing) in the absence/presence of two commercial sealing gaskets (Teflon and silicone gaskets). The following are the main findings of the study:

- The tested GDL materials are expectedly less deformed in the presence of the gaskets. They are also sensitive to the type of the gasket: they are less deformed with silicone gaskets than with Teflon gaskets and this is due to higher stiffness of the former type of gaskets.
- The reduction in the gas permeability and the thickness of the tested GDL materials with Teflon gaskets are higher than that with the silicone gasket and this is evidently relatively higher stiffness of the latter gaskets.

- The MPL-coated GDL samples feature more reduction in their gas permeability and thickness compared to the corresponding bare carbon substrates; this is due to the penetration of the MPLs into the body of the carbon substrates as a result of compression.
- The TGA data shows the PTFE loading of the tested carbon substrates, either without or with gaskets, reduces by about 40% after performing the compression test indicating that some PTFE material is stripped off as a result of the applied compressive forces. The MPL-coated GDLs behave differently as they appear to lose no PTFE material after compression.
- The GDL samples, subject to compression, shows less weight loss after 600 °C compared to uncompressed samples and this is most likely due to presence of less binding materials that are probably lost due to compression. This is corroborated by the observation that more weight loss is observed for the GDL samples compressed along with silicone gaskets that are mechanically stronger than the Teflon gaskets.

Acknowledgements

The first author would like to acknowledge and appreciate the financial support from the Kuwait Institute for Scientific Research (KISR).

References

[1] V. Gurau, M. J. Bluemle, E. S. De Castro, Y. Tsou, T. A. Zawodzinski, and J. A. Mann, "Characterization of transport properties in gas diffusion layers for proton exchange membrane fuel cells: 2. Absolute permeability," vol. 165, pp. 793–802, 2007, doi: 10.1016/j.jpowsour.2006.12.068.

[2] C. Robin, M. Gerard, A. A. Franco, and P. Schott, "Multi-scale coupling between two dynamical models for PEMFC aging prediction," *Int. J. Hydrogen Energy*, vol. 38, no. 11, pp. 4675–4688, 2013, doi: 10.1016/j.ijhydene.2013.01.040.

[3] P. R. Pathapati, X. Xue, and J. Ã. Tang, "A new dynamic model for predicting transient phenomena in a PEM fuel cell system," vol. 30, pp. 1–22, 2005, doi: 10.1016/j.renene.2004.05.001.

[4] E. Carcadea, M. Varlam, M. Ismail, D.B. Ingham, A. Marinoiu, M. Raceanu, C. Jianu, L. Patularu, D. Ion-Ebrasu, "PEM fuel cell performance improvement through numerical optimization of the parameters of the porous layers," *Int. J. Hydrogen Energy*, vol. 45, no. 14, pp. 7968–7980, 2020, doi: 10.1016/j.ijhydene.2019.08.219.

[5] E. Nishiyama and T. Murahashi, "Water transport characteristics in the gas diffusion media of proton exchange membrane fuel cell - Role of the microporous layer," *J. Power Sources*, vol. 196, no. 4, pp. 1847–1854, 2011, doi: 10.1016/j.jpowsour.2010.09.055.

[6] R. Li, Y. Cai, U. Reimer, and K. Wippermann, "CrN / Cr-Coated Steel Plates for High-Temperature Polymer Electrolyte Fuel Cells: Performance and Durability CrN / Cr-Coated Steel Plates for High-Temperature Polymer Electrolyte Fuel Cells: Performance and Durability," 2020, doi: 10.1149/1945-7111/abc76c.

[7] J. Park, H. Oh, T. Ha, Y. Il Lee, and K. Min, "A review of the gas diffusion layer in proton exchange membrane fuel cells: Durability and degradation," *Appl. Energy*, vol. 155, pp. 866–880, 2015, doi: 10.1016/j.apenergy.2015.06.068.

[8] W. R. Chang, J. J. Hwang, F. B. Weng, and S. H. Chan, "Effect of clamping pressure on the performance of a PEM fuel cell," *J. Power Sources*, vol. 166, no. 1, pp. 149–154, 2007, doi: 10.1016/j.jpowsour.2007.01.015.

[9] W. K. Lee, C. H. Ho, J. W. Van Zee, and M. Murthy, "The effects of compression and gas diffusion layers on the performance of a PEM fuel cell," *J. Power Sources*, vol. 84, no. 1, pp. 45–51, 1999, doi: Doi 10.1016/S0378-7753(99)00298-0.

[10] J. Ge, A. Higier, and H. Liu, "Effect of gas diffusion layer compression on PEM fuel cell performance," *J. Power Sources*, vol. 159, no. 2, pp. 922–927, 2006, doi: 10.1016/j.jpowsour.2005.11.069.

[11] T. J. Mason, J. Millichamp, T. P. Neville, P. R. Shearing, S. Simons, and D. J. L. Brett, "A study of the effect of water management and electrode flooding on the dimensional change of polymer electrolyte fuel cells," *J. Power Sources*, vol. 242, no. September 2015, pp. 70–

77, 2013, doi: 10.1016/j.jpowsour.2013.05.045.

[12] T. Ous and C. Arcoumanis, “Effect of compressive force on the performance of a proton exchange membrane fuel cell,” *Proc. Inst. Mech. Eng. Part C J. Mech. Eng. Sci.*, vol. 221, no. 9, pp. 1067–1074, 2007, doi: 10.1243/09544062JMES654.

[13] P. Zhou, C. W. Wu, and G. J. Ma, “Influence of clamping force on the performance of PEMFCs,” *J. Power Sources*, vol. 163, no. 2, pp. 874–881, 2007, doi: 10.1016/j.jpowsour.2006.09.068.

[14] J. Zhang, H. Zhang, J. Wu, J. Zhang, “Design and Fabrication of PEM Fuel Cell MEA, Single Cell, and Stack,” *Pem Fuel Cell Test. Diagnosis*, pp. 43–80, Jan. 2013, doi: 10.1016/B978-0-444-53688-4.00002-4.

[15] F. J. Luczak and S. Sarangapani, “Experimental Methods In Low Temperature Fuel Ccells BT - Fuel Cells: From Fundamentals to Applications,” S. Srinivasan, Ed. Boston, MA: Springer US, 2006, pp. 267–308.

[16] D. Qiu, L. Peng, P. Yi, X. Lai, H. Janßen, and W. Lehnert, “Contact behavior modelling and its size effect on proton exchange membrane fuel cell,” *J. Power Sources*, vol. 365, pp. 190–200, 2017, doi: 10.1016/j.jpowsour.2017.08.088.

[17] H. Tang, Z. Qi, M. Ramani, and J. F. Elter, “PEM fuel cell cathode carbon corrosion due to the formation of air/fuel boundary at the anode,” *J. Power Sources*, vol. 158, no. 2 SPEC. ISS., pp. 1306–1312, 2006, doi: 10.1016/j.jpowsour.2005.10.059.

[18] G. Li, J. Tan, and J. Gong, “Degradation of the elastomeric gasket material in a simulated and four accelerated proton exchange membrane fuel cell environments,” *J. Power Sources*, vol. 205, pp. 244–251, 2012, doi: 10.1016/j.jpowsour.2011.06.092.

[19] J. Tan, Y. J. Chao, J. W. Van Zee, and W. K. Lee, “Degradation of elastomeric gasket materials in PEM fuel cells,” *Mater. Sci. Eng. A*, vol. 445–446, pp. 669–675, 2007, doi: 10.1016/j.msea.2006.09.098.

[20] P. C. Ghosh, “Influences of Contact Pressure on the Performances of Polymer Electrolyte Fuel Cells,” *J. Energy*, vol. 2013, pp. 1–11, 2013, doi: 10.1155/2013/571389.

[21] J. H. Lin, W. H. Chen, Y. J. Su, and T. H. Ko, “Effect of gas diffusion layer compression on the performance in a proton exchange membrane fuel cell,” *Fuel*, vol. 87, no. 12, pp. 2420–2424, 2008, doi: 10.1016/j.fuel.2008.03.001.

[22] R. Banerjee, J. Hinebaugh, H. Liu, R. Yip, N. Ge, and A. Bazylak, “Heterogeneous porosity distributions of polymer electrolyte membrane fuel cell gas diffusion layer materials with rib-channel compression,” *Int. J. Hydrogen Energy*, vol. 1, no. 416, pp. 0–11, 2016, doi: 10.1016/j.ijhydene.2016.06.147.

[23] I. Nitta, O. Himanen, and M. Mikkola, “Thermal conductivity and contact resistance of compressed gas diffusion layer of PEM fuel cell,” *Fuel Cells*, vol. 8, no. 2, pp. 111–119,

2008, doi: 10.1002/fuce.200700054.

[24] F. Aldakheel, M.S. Ismail, K.J. Hughes. D.B. Ingham, L. Ma, M. Pourkashanian, D. Cumming, and R. Smith, "Gas permeability, wettability and morphology of gas diffusion layers before and after performing a realistic ex-situ compression test," *Renew. Energy*, vol. 151, pp. 1082–1091, 2020, doi: 10.1016/j.renene.2019.11.109.

[25] R. R. Rashapov, J. Unno, and J. T. Gostick, "Characterization of PEMFC Gas Diffusion Layer Porosity," *J. Electrochem. Soc.*, vol. 162, no. 6, pp. F603–F612, 2015, doi: 10.1149/2.0921506jes.

[26] Y. Faydi, R. Lachat, and Y. Meyer, "Thermomechanical characterisation of commercial Gas Diffusion Layers of a Proton Exchange Membrane Fuel Cell for high compressive pre-loads under dynamic excitation," *Fuel*, vol. 182, pp. 124–130, 2016, doi: 10.1016/j.fuel.2016.05.074.

[27] J. C. Tsai and C. K. Lin, "Effect of PTFE content in gas diffusion layer based on Nafion®/PTFE membrane for low humidity proton exchange membrane fuel cell," *J. Taiwan Inst. Chem. Eng.*, vol. 42, no. 6, pp. 945–951, 2011, doi: 10.1016/j.jtice.2011.05.008.

[28] T. Ha., J. Cho, J. Park, K. Min, H.S. Kim, E. Lee, and J.Y. Jyoung, "Experimental study of the effect of dissolution on the gas diffusion layer in polymer electrolyte membrane fuel cells," *Int. J. Hydrogen Energy*, vol. 36, no. 19, pp. 12427–12435, 2011, doi: 10.1016/j.ijhydene.2011.06.096.

[29] S. Shukla, F. Wei, M. Mandal, J. Zhou, M.S. Saha, J. Stumper, and M. Secanell, "Determination of PEFC Gas Diffusion Layer and Catalyst Layer Porosity Utilizing Archimedes Principle," *J. Electrochem. Soc.*, vol. 166, no. 15, pp. F1142–F1147, 2019, doi: 10.1149/2.0251915jes.

[30] "Sigracet 34 and 35 Series Carbon Paper GDL Properties Sheet." https://www.fuelcellstore.com/spec-sheets/SGL-GDL_34-35.pdf.

[31] M. S. Ismail, A. Hassanpour, D. B. Ingham, L. Ma, and M. Pourkashanian, "On the compressibility of gas diffusion layers in proton exchange membrane fuel cells," *Fuel Cells*, vol. 12, no. 3, pp. 391–397, 2012, doi: 10.1002/fuce.201100054.

[32] V. V. Atrazhev, T. Y. Astakhova, D.V. Dmitriev, N.S. Erikhman, V.I Sultanov, T.P. Patterson, and S.F. Burlatsky, "The Model of Stress Distribution in Polymer Electrolyte Membrane," *J. Electrochem. Soc.*, vol. 160, no. 10, pp. F1129–F1137, 2013, doi: 10.1149/2.079310jes.

[33] M. S. Ismail, D. Borman, T. Damjanovic, D. B. Ingham, and M. Pourkashanian, "On the through-plane permeability of microporous layer-coated gas diffusion layers used in proton exchange membrane fuel cells," *Int. J. Hydrogen Energy*, vol. 36, no. 16, pp. 10392–10402, 2010, doi: 10.1016/j.ijhydene.2010.09.012.

[34] M. S. Ismail, T. Damjanovic, K. Hughes, D.B. Ingham, L. Ma, M. Pourkashanian, and M.

Rosli, “Through-Plane Permeability for Untreated and PTFE-Treated Gas Diffusion Layers in Proton Exchange Membrane Fuel Cells,” *J. Fuel Cell Sci. Technol.*, vol. 7, no. 5, p. 051016, 2010, doi: 10.1115/1.4000685.

[35] O. M. Orogbemi, D. B. Ingham, M. S. Ismail, K. J. Hughes, L. Ma, and M. Pourkashanian, “The effects of the composition of microporous layers on the permeability of gas diffusion layers used in polymer electrolyte fuel cells,” *Int. J. Hydrogen Energy*, vol. 41, no. 46, pp. 21345–21351, 2016, doi: 10.1016/j.ijhydene.2016.09.160.

[36] O. M. Orogbemi, D. B. Ingham, M. S. Ismail, K. J. Hughes, L. Ma, and M. Pourkashanian, “Through-plane gas permeability of gas diffusion layers and microporous layer: Effects of carbon loading and sintering,” *J. Energy Inst.*, vol. 91, no. 2, pp. 270–278, 2018, doi: 10.1016/j.joei.2016.11.008.

[37] O. M. Orogbemi, D. B. Ingham, M. S. Ismail, K. J. Hughes, L. Ma, and M. Pourkashanian, “On the gas permeability of the microporous layer used in polymer electrolyte fuel cells,” *J. Energy Inst.*, vol. 41, no. 46, pp. 21345–21351, 2017, doi: doi: 10.1016/j.joei.2017.09.006.

[38] H. Pang, P. Huang, W. Zhuo, M. Li, C. Gao, and D. Guo, “Hysteresis and its impact on characterization of mechanical properties of suspended monolayer molybdenum-disulfide sheets,” *Phys. Chem. Chem. Phys.*, vol. 21, no. 14, pp. 7454–7461, 2019, doi: 10.1039/c8cp07158f.

[39] S. Yu, X. Li, J. Li, S. Liu, W. Lu, Z. Shao, and B. Yi, “Study on hydrophobicity degradation of gas diffusion layer in proton exchange membrane fuel cells,” *Energy Convers. Manag.*, vol. 76, pp. 301–306, 2013, doi: 10.1016/j.enconman.2013.07.034.

[40] Y. Ira, Y. Bakhshan, and J. Khorshidimalahmadi, “Effect of wettability heterogeneity and compression on liquid water transport in gas diffusion layer coated with microporous layer of PEMFC,” *Int. J. Hydrogen Energy*, no. xxxx, 2020, doi: 10.1016/j.ijhydene.2021.02.160.

[41] M. S. Ismail, T. Damjanovic, D. B. Ingham, L. Ma, and M. Pourkashanian, “Effect of polytetrafluoroethylene-treatment and microporous layer-coating on the in-plane permeability of gas diffusion layers used in proton exchange membrane fuel cells,” *J. Power Sources*, vol. 195, no. 19, pp. 6619–6628, 2010, doi: 10.1016/j.jpowsour.2010.04.036.